DNA AND CELL BIOLOGY
Volume 40, Number 1, 2021

Pp. 1–8
DOI: 10.1089/dna.2020.6030

S100A2 Silencing Relieves Epithelial–Mesenchymal Transition in Pulmonary Fibrosis by Inhibiting the Wnt/β-Catenin Signaling Pathway

Guichuan Huang,[1] Jing Zhang,[2] Gang Qing,[1] Daishun Liu,[3] Xin Wang,[1] Yi Chen,[1] Yishi Li,[1] and Shuliang Guo[1]

Pulmonary fibrosis (PF) is a progressive and lethal disease with poor prognosis. *S100A2* plays an important role in the progression of cancer. However, the role of *S100A2* in PF has not yet been reported. In this study, we explored the potential role of *S100A2* in PF and its potential molecular mechanisms. Increased expression of *S100A2* was first observed in lung tissues of PF patients. We found that downregulation of *S100A2* inhibited the transforming growth factor-β1 (TGF-β1)-induced epithelial–mesenchymal transition (EMT) in A549 cells. Mechanically, TGF-β1 upregulated β-catenin and the phosphorylation of glycogen synthase kinase-3β, which was blocked by silencing *S100A2 in vitro*. Furthermore, lithium chloride (activator of the Wnt/β-catenin signaling pathway) effectively rescued *S100A2* knockdown-mediated inhibition of EMT in PF. In conclusion, these findings demonstrate that downregulation of *S100A2* alleviated PF through inhibiting EMT. *S100A2* is a promising potential target for further understanding the mechanism and developing a strategy for the treatment of PF and other EMT-associated diseases.

Keywords: pulmonary fibrosis, epithelial–mesenchymal transition, *S100A2*, transforming growth factor-β1

Introduction

Pulmonary fibrosis (PF) is a common outcome of various interstitial lung diseases, including coronavirus disease-2019 (COVID-19), pneumoconiosis, drug-induced fibrosis, and idiopathic PF (Du *et al.*, 2019; George *et al.*, 2020; He *et al.*, 2020). PF is characterized by alveolar epithelial cell (AEC) injury, and the excessive proliferation of mesenchymal cells in the interstitium, which leads to the exaggerated accumulation of extracellular matrix (ECM) and distorted lung architecture. Although we have made great progress in the diagnosis of and treatment for PF in recent years, the survival rate has not improved (Kumar *et al.*, 2018). Therefore, it is crucial to explore the precise molecular mechanisms involved in the development of PF and to determine targets for the diagnosis and treatment of PF.

Epithelial–mesenchymal transition (EMT) is a process in which epithelial cells are transformed into a mesenchymal phenotype, with the loss of contact adhesion and apical–basal polarity, acquisition of the mesenchymal property of invasion, migration, and production of ECM (Jolly *et al.*, 2018). An increasing number of studies have shown that EMT plays an important role in the pathogenesis of PF (Salton *et al.*, 2019). In addition, transforming growth factor-β1 (TGF-β1) is a key profibrotic factor that has been implicated to induce EMT during PF (Willis and Borok, 2007).

The S100 protein family is a group of highly conserved elongation factor (EF)-hand calcium-binding proteins (Chen *et al.*, 2014). *S100A2* is an important member of the S100 protein family and has been involved in various cancers (Wolf *et al.*, 2011). Naz *et al.* (2014) reported that *S100A2* promoted the occurrence of cancer through regulating PI3K/Akt signaling and the functional interaction with Smad3. In addition, a study indicated that the p53-*S100A2* positive feedback loop negatively regulates epithelialization in cutaneous wound healing (Pan *et al.*, 2018). However, the role of *S100A2* in fibrosis, including PF, has not been investigated.

In this study, we demonstrated that *S100A2* was increased in lung tissues of patients with PF. Downregulation of *S100A2* inhibited TGF-β1-induced EMT in human type II AECs through blocking the Wnt/β-catenin pathway *in vitro*. These results will increase our understanding of the pathological mechanisms of PF.

[1]Department of Pulmonary and Critical Care Medicine, The First Affiliated Hospital of Chongqing Medical University, Chongqing, China.
[2]Department of Pulmonary and Critical Care Medicine, Affiliated Hospital of Zunyi Medical University, Zunyi, China.
[3]Zunyi Medical University, Zunyi, China.

Materials and Methods

Ethics statement

The study was approved by the ethics committee of The First Affiliated Hospital of Chongqing Medical University (No. 2020-147), and the study was in accordance with the Declaration of Helsinki.

Data collection from the Gene Expression Omnibus database

We searched microarray data of *S100A2* in the Gene Expression Omnibus (GEO) database (www.ncbi.nlm.nih.gov/geo). The following keywords were used: (lung fibrosis OR pulmonary fibrosis). The search results were further restricted as following: Series [Entry type] and *Homo sapiens* [Organism]. Inclusion criteria for microarrays were as follows: (1) the data set included fibrotic and nonfibrotic tissues; (2) the number of samples in fibrotic and nonfibrotic tissues was at least two; (3) data set provided the expression values of *S100A2* in fibrotic and nonfibrotic tissues.

Tissues, cell line, and cell culture

Twelve PF tissues were obtained from patients undergoing lung biopsy. A total of 17 control lung tissues were collected from the normal areas of the peripheral lung removed during lung cancer resection. All tissues were obtained from the First Affiliated Hospital of Chongqing Medical University.

The human type II AEC line, A549, was purchased from the Cell Bank of the Chinese Academy of Sciences. Cells were cultured in Roswell Park Memorial Institute-1640 (RPMI-1640) medium supplemented with 10% fetal calf serum (PAN), 100 U/mL penicillin, and 100 μg/mL streptomycin (Gibco) at 37°C in a 5% carbon dioxide atmosphere. A549 cells were treated with recombinant human TGF-β1 (Peprotech, NJ) at final concentration of 10 ng/mL for 48 h with or without 20 mmol/L lithium chloride (LiCl; an agonist of the Wnt/β-catenin signaling pathway) (Sigma, USA). Then, the cells were collected for further analysis.

Lentivirus transfection

To establish stable genetic silencing of *S100A2*, lentivirus was utilized as a vector to carry the interference sequence. The lentivirus vectors inserted with the target gene or a negative control were constructed by Hanbio Biotechnology Company (Shanghai, China). Then, lentivirus was added to 2 mL complete medium supplemented with a final concentration of 5 μg/mL Polybrene. After 24 h, the medium was replaced with fresh complete medium without lentivirus and Polybrene to culture for another 48 h. Total RNA and protein were collected to confirm the transfection efficiency using quantitative real-time PCR (qRT-PCR) and Western blot.

Quantitative real-time PCR

Total RNA was extracted from the lung tissues or A549 cells using TRIzol reagent (Invitrogen, Carlsbad, CA). The concentration of RNA was measured with the use of the NanoDrop 2000 spectrophotometer (Thermo Scientific, Waltham, MA). Then, 1000 ng of total RNA was reverse transcribed using the PrimeScript RT reagent kit (TaKaRa, Dalian, China). Subsequently, cDNA was amplified by SYBR Premix Ex Taq (TaKaRa). The relative expression levels of mRNA were normalized to the levels of GAPDH and calculated by the $2^{-\triangle\triangle CT}$ method. The primers used in this study are listed as follows: α-smooth muscle actin (α-SMA), forward, 5′-ATGCTCCCAGGGCTGTTTTC-3′, reverse, 5′-CTTTTGCTCTGTGCTTCGTC-3′; *S100A2*, forward, 5′-ACCGACCC TGAAGCAGAACTC-3′, reverse, 5′-CCTCA TCTCCCAGCACTCCA-3′; E-cadherin, forward, 5′-CGATTC AAAGTGGGCACAGATG-3′, reverse, 5′-GTAGG TGGAGT CCCAGGCGTAG-3′; vimentin, forward, 5′-TCTGGATTCAC TCCCTCT GGTT-3′, reverse, 5′-ATCGTGATGCTGAGAAG TTTCGT-3′, and GAPDH, forward, 5′-CTTTGGTA TCGTGG AAGGACTC-3′, reverse, 5′-GTAGAGGCAGG GATGATG TTCT-3′.

Enzyme-linked immunosorbent assay

The concentration of E-cadherin, vimentin, and α-SMA in the culture medium without dilution was measured using an enzyme-linked immunosorbent assay Kit (Jingmei Biotech., China) according to the manufacturer's protocol.

Hematoxylin and eosin staining

For hematoxylin and eosin (H&E) staining analysis, 5 μm thick sections of lung tissue were deparaffinized in xylene followed by subjecting to rehydration using an ethanol gradient. The slices were stained with hematoxylin for several minutes. The 70% and 90% ethanol were used to dehydrate. Finally, the slices were stained with eosin for few minutes and observed under an Olympus microscope.

Immunohistochemistry

For immunohistochemistry analysis, 5 μm thick sections of lung tissue were deparaffinized in xylene followed by subjecting to rehydration using an ethanol gradient. Next, the endogenous peroxide activity was blocked using 3% hydrogen peroxide. After blocking with 5% BSA, the sections were incubated with primary anti-*S100A2* (1:400; Abcam) antibodies overnight at 4°C. Subsequently, the sections were incubated with horseradish peroxidase-conjugated goat antirabbit IgG (Abcam) for 1 h at room temperature. The sections were developed with the use of diaminobenzidine. The sections were visualized for immunopositivity and images were captured using an Olympus microscope.

Western blot

Cells were lysed in radioimmunoprecipitation assay lysis buffer containing protease inhibitor cocktail, 1% phenylmethanesulfonyl fluoride, and 1% phosphatase inhibitor. Protein concentration was determined with a bicinchoninic acid kit (Beyotime, Biotechnology, China). Equal amounts of protein were separated with 10% sodium dodecyl sulfate-polyacrylamide gel electrophoresis (SDS-PAGE) gel and transferred to polyvinylidene fluoride membranes. After blocking in 5% nonfat milk for 2 h, the membranes were incubated with primary antibodies overnight at 4°C. Then, the membranes were incubated in tris-buffered saline with tween 20 (TBST) supplemented with secondary antibody for 1 h at room temperature. In this experiment, the following antibodies were used: anti-p-glycogen synthase kinase-3β (p-GSK3β) (1:1000; Affinity Biosciences), anti-GSK3β (1:500; Affinity Biosciences),

anti-E-cadherin (1:10,000; Abcam), anti-vimentin (1:3000; Abcam), anti-α-SMA (1:2000; Abcam), anti-*S100A2* (1:5000; Abcam), anti-GAPDH (1:10,000; Abcam), and anti-β-catenin (1:5000; Abcam).

Statistical Analysis

Statistical analyses were performed with SPSS 24.0. All data are expressed as the mean ± standard deviation. The data were analyzed using independent samples Student's *t*-test between two groups and one-way analysis of variance for more groups with Dunnett's or least significant difference (LSD) *post hoc* test.

We carried out a comprehensive meta-analysis using STATA 12.0. Continuous outcomes are presented as the standard mean difference (SMD) with 95% confidence interval (CI). The chi-squared test and I^2 were used to evaluate the heterogeneity among the studies. A random-effect model was applied if there was heterogeneity among the studies ($I^2 > 50\%$ or $p_{heterogeneity} < 0.05$). On the contrary, if $I^2 < 50\%$ or $p_{heterogeneity} > 0.05$, a fixed-effect model was employed. A value of $p < 0.05$ was considered statistically significant.

Results

S100A2 *expression was increased in PF obtained from GEO database*

A total of 14 GEO series (GSE) from National Center for Biotechnology Information's (NCBI's) GEO database met the inclusion criteria. However, only eight GSE data sets provided the *S100A2* expression data. As shown in Supplementary Table S1, the detailed information for *S100A2* expression data from the PF and control groups was extracted based on the GEO database. A total of 168 patients with PF were included. As shown in Figure 1, compared with the control groups, PF groups had a significantly higher expression level of *S100A2* in accession

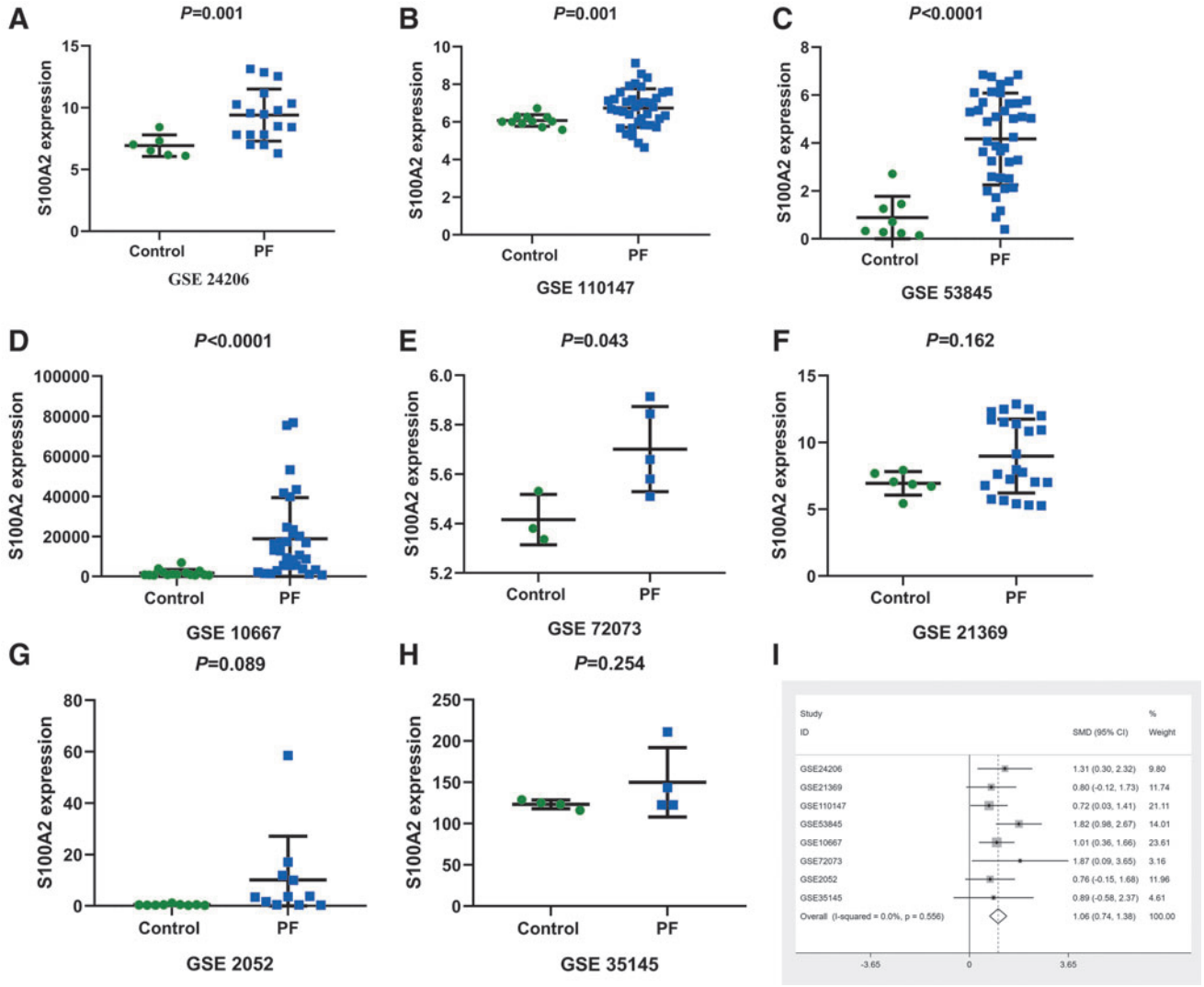

FIG. 1. Expression levels of *S100A2* in PF and control lung tissues from the GEO database. **(A)** GSE24206, **(B)** GSE110147, **(C)**, GSE53845, **(D)**, GSE10667, **(E)**, GSE72073, **(F)**, GSE21369, **(G)**, GSE2052, **(H)**, GSE35145, and **(I)** meta-analysis for all data sets. CI, confidence interval; GEO, Gene Expression Omnibus; PF, pulmonary fibrosis.

numbers GSE24206, GSE110147, GSE53845, GSE10667, and GSE72073. Although no statistical differences were observed in the *S100A2* expression level between the PF groups and control groups in GSE21369, GSE2052, and GSE35145 (Fig. 1F–H), we found that the PF groups also exhibited higher *S100A2* expression than the control groups.

Different results existed regarding *S100A2* expression in PF based on the GEO database. Thus, we conducted a meta-analysis using the data for the *S100A2* expression level from the GEO database. Owing to $I^2 = 0.0\%$ and $p_{heterogeneity} > 0.05$, a fixed model was applied. As shown in Figure 1I, the combined results revealed that the expression of *S100A2* was significantly higher in the PF group than in the control group (SMD = 1.06, 95% CI: 0.74–1.38, $p < 0.001$).

Validation of differential S100A2 *expression in PF in humans both* in vivo *and* in vitro

To further confirm the differential expression of *S100A2* during lung fibrosis, we compared its expression in lung fibrosis tissues from PF patients ($n = 12$) with the control ($n = 17$). The detailed information for PF patients is listed in Supplementary Table S2.

The H&E staining was used to assess histopathological changes of lung tissue. As shown in Figure 2A and B, the control groups showed that clear alveolar space structure and alveolar interval thickness, whereas inflammatory cell infiltration, widened alveolar spaces, and the formation of fibrotic foci were observed in PF patients. As shown in Figure 2E, qRT-PCR indicated that the expression of *S100A2* in lung tissues was significantly increased in PF patients, as compared with control groups ($p < 0.001$). Furthermore, immunohistochemistry indicated that the expression of *S100A2* was increased in PF tissue (Fig. 2C, D). In addition, we examined *S100A2* expression in A549 cells after TGF-β1 treatment. As shown in Figure 2F, the mRNA expression of *S100A2* was significantly increased in TGF-β1-stimulated A549 cells. Furthermore, the *S100A2* expression in A549 was also evaluated by Western blot analysis (Fig. 2G, H). The *S100A2* protein was obviously overexpressed in A549 cells that

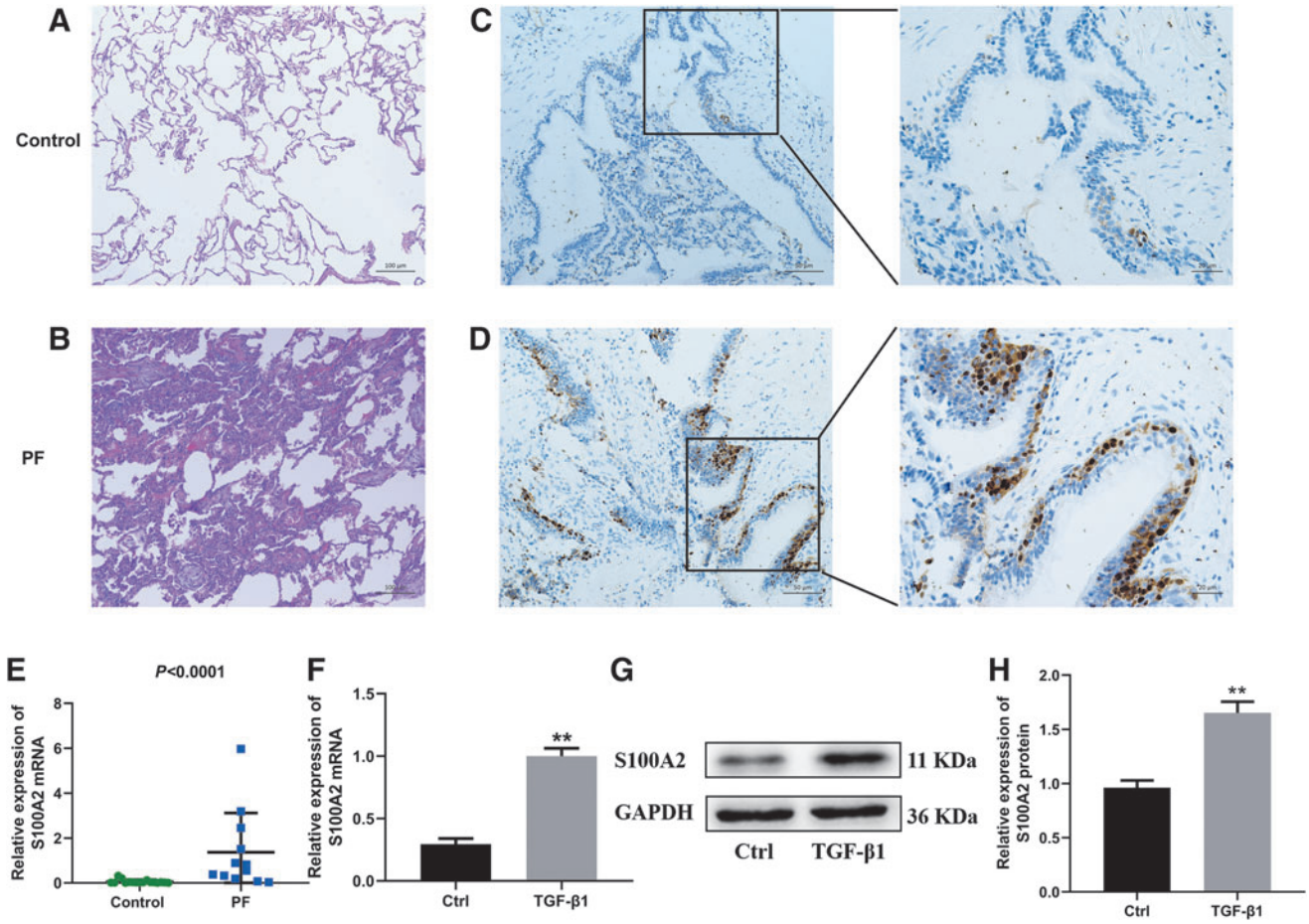

FIG. 2. Expression of *S100A2* in human PF tissues and human pulmonary epithelial cells (A549) treated with TGF-β1. **(A, B)** Lung tissues were conducted with H&E staining (original magnification × 100, scale bar: 100 μm). **(C, D)** The protein expression of *S100A2* in human PF tissues and in normal human lung tissues detected by immunohistochemistry (original magnification × 200, scale bar: 50 μm; original magnification × 400, scale bar: 20 μm). **(E)** The mRNA expression of *S100A2* in human PF tissues and in normal human lung tissues detected by qRT-PCR. A549 cells were treated with or without TGF-β1 for 48 h. **(F)** The mRNA expression of *S100A2* was determined by qRT-PCR. **(G, H)** The protein expression of *S100A2* was measured by Western blot. Data are shown as the mean ± SD ($n = 3$). $^{**}p < 0.01$ versus Ctrl. Ctrl, control; H&E, hematoxylin and eosin; qRT-PCR, quantitative real-time PCR; SD, standard deviation; TGF-β1, transforming growth factor-β1.

received TGF-β1 treatment. Taken together, these findings indicated that *S100A2* was upregulated both in PF tissues and in A549 cells treated with TGF-β1.

Downregulation of S100A2 *inhibits TGF-β1-induced EMT in A549 cells*

EMT is characterized by the loss of the epithelial cell marker E-cadherin and overexpression of the mesenchymal markers vimentin and α-SMA. TGF-β1 is one of the key regulators of PF and induces EMT of AECs *in vitro* (Kasai *et al.*, 2005). To investigate the effect of *S100A2* on TGF-β1-stimulated EMT in A549 cells, *S100A2* gene expression knockdown was performed in A549 cells and then stimulated with TGF-β1. First, the knockdown efficiency of *S100A2* was measured with the use of qRT-PCR and Western blot assay. As shown in Supplementary Figure S1, the mRNA and protein expression of *S100A2* was dramatically downregulated in the short harpin RNA (shRNA)-*S100A2* group compared with the shRNA-negative control group. Downregulation of *S100A2* obviously increased TGF-β1-induced expression of E-cadherin and reduced the expression of vimentin and α-SMA in A549 cells both at the mRNA and protein level (Fig. 3A–H), suggesting that *S100A2* knockdown inhibited TGF-β1-induced EMT.

Deletion of S100A2 *suppresses TGF-β1-induced EMT in A549 cells through the Wnt/β-catenin signaling pathway*

GSK-3β and β-catenin are two key molecules in the Wnt/β-catenin signaling pathway. We used silencing of *S100A2*

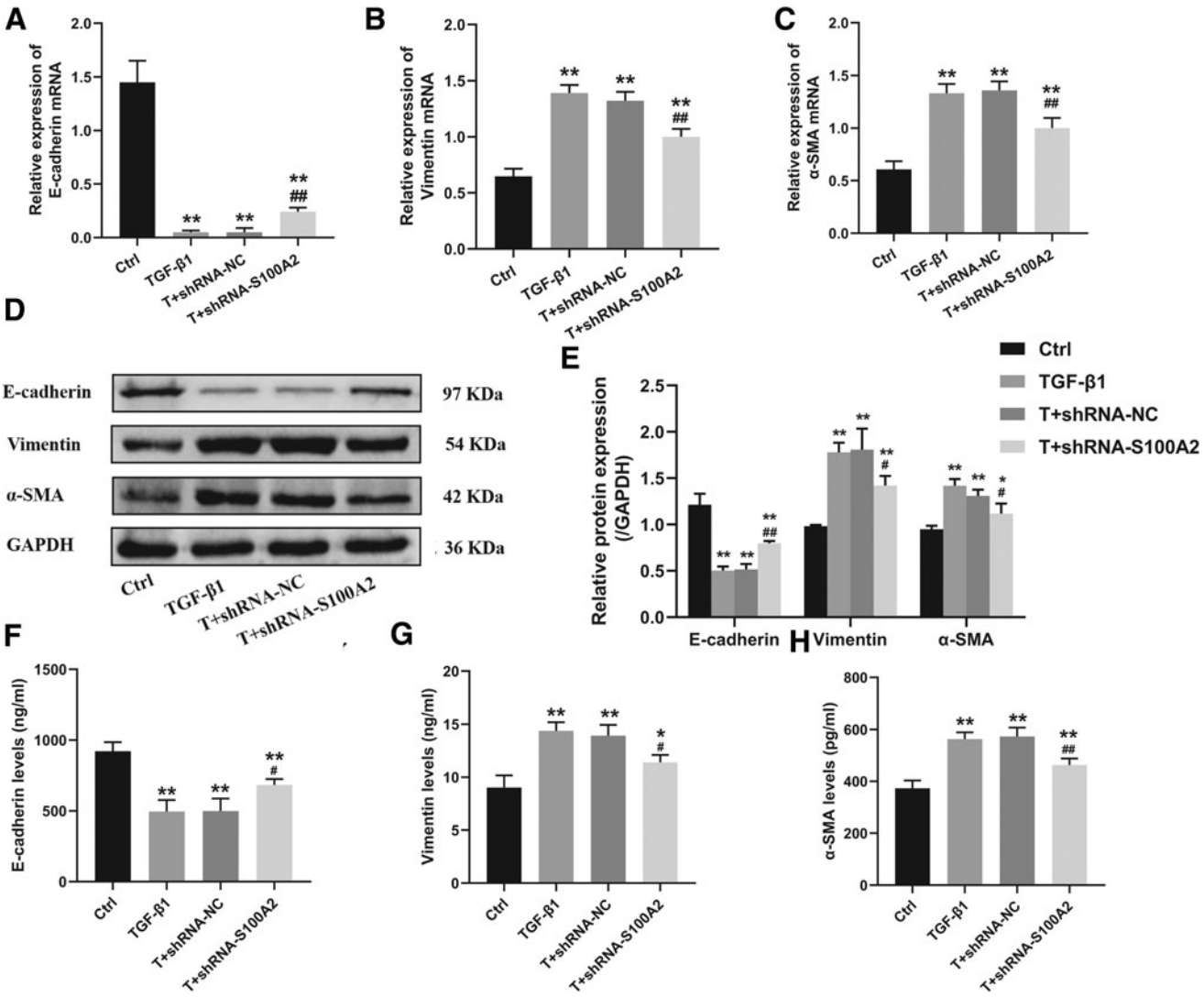

FIG. 3. Effect of *S100A2* on TGF-β1-induced EMT. A549 cells were exposed to 10 ng/mL TGF-β1 stimulation for 48 h. The mRNA of E-cadherin **(A)**, vimentin **(B)**, and α-SMA **(C)** was measured using qRT-PCR. The protein of E-cadherin, vimentin, and α-SMA was detected by Western blot **(D, E)**. The concentration of E-cadherin, vimentin, and α-SMA in the culture medium without dilution was measured using an enzyme-linked immunosorbent assay kit **(F–H)**. Data are shown as the mean ± SD ($n = 3$). $^{*}p < 0.05$ versus Ctrl; $^{**}p < 0.01$ versus Ctrl. $^{\#}p < 0.05$ versus T+shRNA-NC; $^{\#\#}p < 0.01$ versus T+shRNA-NC. α-SMA, α-smooth muscle actin; EMT, epithelial–mesenchymal transition; shRNA-NC, short harpin RNA-negative control; shRNA-*S100A2*, short harpin RNA-*S100A2*; T, TGF-β1.

to determine whether *S100A2* mediated TGF-β1-induced EMT through the Wnt/β-catenin pathway. A549 cells were treated with TGF-β1, and β-catenin/GSK-3β protein expression levels were detected using Western blot. Knockdown of *S100A2* suppressed TGF-β1-induced β-catenin and phosphorylation of GSK-3β, and the protein levels of nonphosphorylated GSK-3β remained unchanged in each group (Fig. 4A–C). These results demonstrated that *S100A2* blocked TGF-β1-induced EMT through downregulation of the β-catenin pathway.

Reactivation of Wnt/β-catenin signaling recovered the suppressive effect of downregulation of S100A2 *on EMT*

Finally, we explored whether *S100A2* exerts its effect on EMT in a Wnt/β-catenin signaling-dependent pathway. LiCl, which is a Wnt/β-catenin signaling pathway activator, was added to A549 cells treated with TGF-β1. As shown in Figure 4D–H, the changes in EMT marker expression (E-cadherin, vimentin, and α-SMA) and β-catenin caused by *S100A2* downregulation can be reversed by LiCl. Collectively, these findings indicated that downregulation of *S100A2* inhibited the EMT of A549 cells by suppressing the Wnt/β-catenin signaling pathway.

Discussion

PF is characterized by progressive dyspnea, and patients eventually die from respiratory failure. The pathologic mechanisms of PF are not completely clear, and effective therapy has not been well developed. Therefore, it is crucial to explore the precise molecular mechanisms involved in the development of PF and to determine a target for treatment of PF.

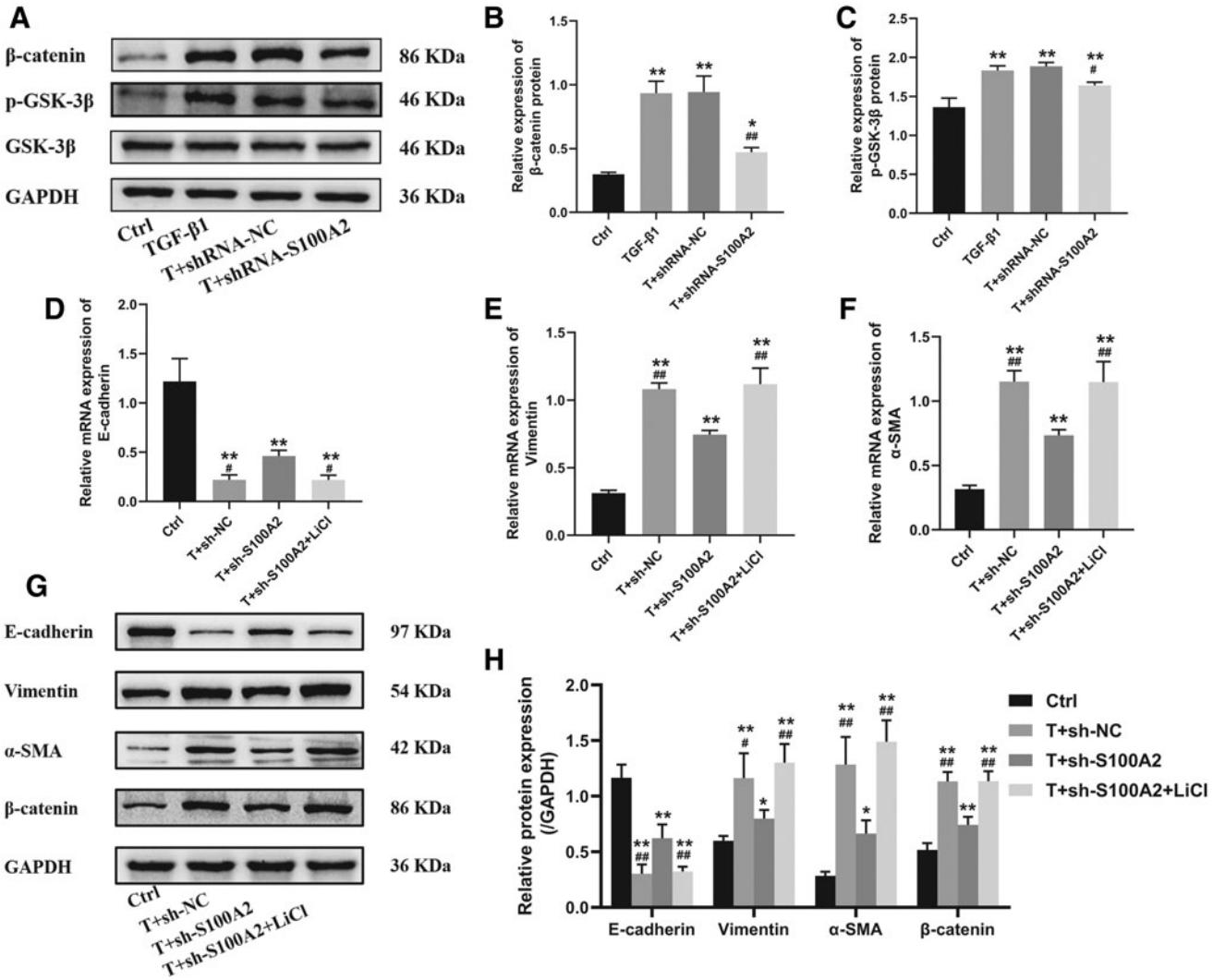

FIG. 4. Downregulation of *S100A2* suppresses EMT through inhibiting the Wnt/β-catenin signaling pathway. The relative protein expression of β-catenin and p-GSK-3β was determined by Western blot **(A–C)**. $^{*}p<0.05$ versus Ctrl; $^{**}p<0.01$ versus Ctrl. $^{\#}p<0.05$ versus T+shRNA-NC; $^{\#\#}p<0.01$ versus T+shRNA-NC. Reactivation of Wnt/β-catenin signaling recovered the suppressive effect of downregulation of *S100A2* on EMT. The relative protein expression of E-cadherin, vimentin, α-SMA, and β-catenin was determined by qRT-PCR **(D–F)** and Western blot **(G, H)**. $^{*}p<0.05$ versus Ctrl; $^{**}p<0.01$ versus Ctrl. $^{\#}p<0.05$ versus T+sh-*S100A2*; $^{\#\#}p<0.01$ versus T+sh-*S100A2*. Data are shown as the mean ± SD ($n=3$). LiCl, lithium chloride.

In this study, we explored the expression, regulation, and potential role of *S100A2* in PF. First, we studied and combined the *S100A2* expression of PF patients from the GEO database. The pooled results from the GEO database showed that the expression of *S100A2* in PF lung tissues was significantly higher than that in normal lung tissues, which demonstrated that *S100A2* may be involved in PF. Furthermore, we confirmed the increased expression of *S100A2* in patients with PF using qRT-PCR and immunohistochemistry assay. Further studies indicated that knockdown of *S100A2* suppressed TGF-β1-induced EMT in A549 cells. Moreover, our study showed that downregulation of *S100A2* inhibited EMT through the Wnt/β-catenin pathway. These findings indicated that *S100A2* was correlated with the development of PF and may serve as a new target for the prevention and treatment of PF.

S100A2 is widely studied in various cancers. Many studies indicate that there is a certain similarity between tumor metastasis and fibrotic diseases. For instance, the dysregulated TGF-β1 pathway and activated EMT process are involved in these two diseases. Downregulation of *S100A2* was detected in gastric cancer and oral squamous cell cancer (Wolf *et al.*, 2011). However, increased *S100A2* expression was observed in ovarian cancer (Hough *et al.*, 2001), bladder cancer (Yao *et al.*, 2007), and nonsmall cell lung cancer (Bulk *et al.*, 2009). In this study, our data showed the first evidence that the expression of *S100A2* was increased in PF lung tissue.

EMT is involved in the pathogenesis of fibrotic diseases in many organs, including the lung. TGF-β1 is considered to be a key profibrotic cytokine and a regulator of EMT. It is well established that AECs, particularly type II AECs, obtain their phenotype of fibroblasts through EMT to contribute to the development of PF (Willis *et al.*, 2005; Kim *et al.*, 2006). Although A549 cell is a cancer cell line, the cells retain the characteristics of type II AECs (Foster *et al.*, 1998; Wu *et al.*, 2017). In addition, AECs are difficult to obtain and maintain in culture *ex vivo*. Therefore, the A549 cell line is usually used as a replacement for primary AECs and is extensively used to study the mechanism of PF (Uhal *et al.*, 2013; Zhu *et al.*, 2016; Liu *et al.*, 2019). In this study, we employed TGF-β1 to build an EMT model using the A549 cell line. In our study, we demonstrated that downregulation of *S100A2* inhibited TGF-β1-induced EMT.

The Wnt/β-catenin signaling pathway plays essential roles in a variety of biological processes, including embryonic axial development, organogenesis, adult stem cell maintenance, and tissue homeostasis (Moon *et al.*, 2004; Brack *et al.*, 2007; Clevers and Nusse, 2012). The key molecule of the pathway is β-catenin. Under normal conditions, β-catenin is phosphorylated by a destruction complex that is composed of axin, GSK-3β, and adenomatous polyposis coli protein, and then ubiquitinated and ultimately destroyed by the proteasome (Guo *et al.*, 2012). Under pathological conditions, Wnt proteins bind to their receptors, and result in the disassembly of the destruction complex, leading to dephosphorylation of β-catenin. Subsequently, β-catenin is allowed to translocate into the nucleus, where it binds to T cell factor/lymphoid enhancer factor, which is in the transcription factor family, to trigger the transcription of β-catenin target genes (Rao and Kühl, 2010). It has been demonstrated that the Wnt/β-catenin signaling pathway plays an important role in the pathological processes involving PF, and suppression of Wnt/β-catenin signaling could inhibit the development of PF (Chilosi *et al.*, 2003; Wang *et al.*, 2014, 2015). GSK-3β is a serine/threonine protein kinase that promotes fibrogenic activity by participating in the execution of Wnt/β-catenin pathway (Beurel *et al.*, 2015; Singh *et al.*, 2015; Boyapally *et al.*, 2019). In this study, we discovered that inhibition of *S100A2* restrains EMT by inhibiting the Wnt/β-catenin pathway.

In conclusion, we demonstrated that the expression of *S100A2* was increased in the lung tissues in patients with PF. Inhibition of *S100A2* can attenuate TGF-β1-induced EMT through inhibiting the β-catenin signaling pathway. *S100A2* is a promising potential target for further understanding the mechanism and developing a strategy for the treatment of PF and other EMT-associated diseases.

Disclosure Statement

The authors declare that they have no conflict of interest.

Funding Information

This research was supported by the National Major Science and Technology Projects of China (Grant No. 2018ZX10 302302003).

Supplementary Material

Supplementary Figure S1
Supplementary Table S1
Supplementary Table S2

References

Beurel, E., Grieco, S.F., and Jope, R.S. (2015). Glycogen synthase kinase-3 (GSK3): regulation, actions, and diseases. Pharmacol Ther **148,** 114–131.

Boyapally, R., Pulivendala, G., Bale, S., and Godugu, C. (2019). Niclosamide alleviates pulmonary fibrosis in vitro and in vivo by attenuation of epithelial-to-mesenchymal transition, matrix proteins & Wnt/beta-catenin signaling: a drug repurposing study. Life Sci **220,** 8–20.

Brack, A.S., Conboy, M.J., Roy, S., Lee, M., Kuo, C.J., Keller, C., *et al.* (2007). Increased Wnt signaling during aging alters muscle stem cell fate and increases fibrosis. Science **317,** 807–810.

Bulk, E., Sargin, B., Krug, U., Hascher, A., Jun, Y., Knop, M., *et al.* (2009). S100A2 induces metastasis in non-small cell lung cancer. Clin Cancer Res **15,** 22–29.

Chen, H., Xu, C., Jin, Q., and Liu, Z. (2014). S100 protein family in human cancer. Am J Cancer Res **4,** 89–115.

Chilosi, M., Poletti, V., Zamo, A., Lestani, M., Montagna, L., Piccoli, P., *et al.* (2003). Aberrant Wnt/beta-catenin pathway activation in idiopathic pulmonary fibrosis. Am J Pathol **162,** 1495–1502.

Clevers, H., and Nusse, R. (2012). Wnt/β-catenin signaling and disease. Cell **149,** 1192–1205.

Du, S., Li, C., Lu, Y., Lei, X., Zhang, Y., Li, S., *et al.* (2019). Dioscin alleviates crystalline silica-induced pulmonary inflammation and fibrosis through promoting alveolar macrophage autophagy. Theranostics **9,** 1878–1892.

Foster, K.A., Oster, C.G., Mayer, M.M., Avery, M.L., and Audus, K.L. (1998). Characterization of the A549 cell line as

a type II pulmonary epithelial cell model for drug metabolism. Exp Cell Res **243,** 359–366.

George, P.M., Wells, A.U., and Jenkins, R.G. (2020). Pulmonary fibrosis and COVID-19: the potential role for antifibrotic therapy. Lancet Respir Med **8,** 807–815.

Guo, Y., Xiao, L., Sun, L., and Liu, F. (2012). Wnt/beta-catenin signaling: a promising new target for fibrosis diseases. Physiol Res **61,** 337–346.

He, F., Wang, Y., Li, Y., and Yu, L. (2020). Human amniotic mesenchymal stem cells alleviate paraquat-induced pulmonary fibrosis in rats by inhibiting the inflammatory response. Life Sci **243,** 117290.

Hough, C.D., Cho, K.R., Zonderman, A.B., Schwartz, D.R., and Morin, P.J. (2001). Coordinately up-regulated genes in ovarian cancer. Cancer Res **61,** 3869–3876.

Jolly, M.K., Ward, C., Eapen, M.S., Myers, S., Hallgren, O., Levine, H., *et al.* (2018). Epithelial-mesenchymal transition, a spectrum of states: role in lung development, homeostasis, and disease. Dev Dyn **247,** 346–358.

Kasai, H., Allen, J.T., Mason, R.M., Kamimura, T., and Zhang, Z. (2005). TGF-beta1 induces human alveolar epithelial to mesenchymal cell transition (EMT). Respir Res **6,** 56.

Kim, K.K., Kugler, M.C., Wolters, P.J., Robillard, L., Galvez, M.G., Brumwell, A.N., *et al.* (2006). Alveolar epithelial cell mesenchymal transition develops in vivo during pulmonary fibrosis and is regulated by the extracellular matrix. Proc Natl Acad Sci U S A **103,** 13180–13185.

Kumar, A., Kapnadak, S.G., Girgis, R.E., and Raghu, G. (2018). Lung transplantation in idiopathic pulmonary fibrosis. Expert Rev Respir Med **12,** 375–385.

Liu, G., Wang, Y., Yang, L., Zou, B., Gao, S., Song, Z., *et al.* (2019). Tetraspanin 1 as a mediator of fibrosis inhibits EMT process and Smad2/3 and beta-catenin pathway in human pulmonary fibrosis. J Cell Mol Med **23,** 3583–3596.

Moon, R.T., Kohn, A.D., De-Ferrari G.V., and Kaykas, A. (2004). WNT and beta-catenin signalling: diseases and therapies. Nat Rev Genet **5,** 691–701.

Naz, S., Bashir, M., Ranganathan, P., Bodapati, P., Santosh, V., and Kondaiah, P. (2014). Protumorigenic actions of S100A2 involve regulation of PI3/Akt signaling and functional interaction with Smad3. Carcinogenesis **35,** 14–23.

Pan, S.C., Li, C.Y., Kuo, C.Y., Kuo, Y.Z., Fang, W.Y., Huang, Y.H., *et al.* (2018). The p53-S100A2 positive feedback loop negatively regulates epithelialization in cutaneous wound healing. Sci Rep **8,** 5458.

Rao, T.P., and Kühl, M. (2010). An updated overview on Wnt signaling pathways: a prelude for more. Circ Res **106,** 1798–1806.

Salton, F., Volpe, M.C., and Confalonieri, M. (2019). Epithelial-mesenchymal transition in the pathogenesis of idiopathic pulmonary fibrosis. Medicina (Kaunas) **55,** 83.

Singh, S.P., Tao, S., Fields, T.A., Webb, S., Harris, R.C., and Rao, R. (2015). Glycogen synthase kinase-3 inhibition attenuates fibroblast activation and development of fibrosis following renal ischemia-reperfusion in mice. Dis Model Mech **8,** 931–940.

Uhal, B.D., Dang, M., Dang, V., Llatos, R., Cano, E., Abdul-Hafez, A., *et al.* (2013). Cell cycle dependence of ACE-2 explains downregulation in idiopathic pulmonary fibrosis. Eur Respir J **42,** 198–210.

Wang, C., Zhu, H., Sun, Z., Xiang, Z., Ge, Y., Ni, C., *et al.* (2014). Inhibition of Wnt/beta-catenin signaling promotes epithelial differentiation of mesenchymal stem cells and repairs bleomycin-induced lung injury. Am J Physiol Cell Physiol **307,** C234-C244.

Wang, X., Dai, W., Wang, Y., Gu, Q., Yang, D., and Zhang, M. (2015). Blocking the Wnt/beta-catenin pathway by lentivirus-mediated short hairpin RNA targeting beta-catenin gene suppresses silica-induced lung fibrosis in mice. Int J Environ Res Public Health **12,** 10739–10754.

Willis, B.C., and Borok, Z. (2007). TGF-beta-induced EMT: mechanisms and implications for fibrotic lung disease. Am J Physiol Lung Cell Mol Physiol **293,** L525–L534.

Willis, B.C., Liebler, J.M., Luby-Phelps, K., Nicholson, A.G., Crandall, E.D., du Bois, R.M., *et al.* (2005). Induction of epithelial-mesenchymal transition in alveolar epithelial cells by transforming growth factor-beta1: potential role in idiopathic pulmonary fibrosis. Am J Pathol **166,** 1321–1332.

Wolf, S., Haase-Kohn, C., and Pietzsch, J. (2011). S100A2 in cancerogenesis: a friend or a foe? Amino Acids **41,** 849–861.

Wu, J., Wang, Y., Liu, G., Jia, Y., Yang, J., Shi, J., *et al.* (2017). Characterization of air-liquid interface culture of A549 alveolar epithelial cells. Braz J Med Biol Res 51:e6950.

Yao, R., Lopez-Beltran, A., Maclennan, G.T., Montironi, R., Eble, J.N., and Cheng, L. (2007). Expression of S100 protein family members in the pathogenesis of bladder tumors. Anticancer Res **27,** 3051–3058.

Zhu, Y., Tan, J., Xie, H., Wang, J., Meng, X., and Wang, R. (2016). HIF-1α regulates EMT via the Snail and β-catenin pathways in paraquat poisoning-induced early pulmonary fibrosis. J Cell Mol Med **20,** 688–697.

Address correspondence to:
Shuliang Guo, PhD
Department of Pulmonary and Critical Care Medicine
The First Affiliated Hospital of Chongqing Medical University
No. 1, Youyi Road
Yuzhong, Chongqing 400016
China

E-mail: guosl999@sina.com

Received for publication August 10, 2020; received in revised form September 25, 2020; accepted October 9, 2020.